

# Thermal Properties of Chitosan-roselle Films

Irwana Nainggolan<sup>1,2\*</sup>, Tulus Ikhsan Nasution<sup>3,2</sup> and Khairel Rafezi Ahmad<sup>4</sup>

<sup>1</sup>Department of Chemistry, Faculty of Mathematics and Natural Sciences, Universitas Sumatera Utara, Medan 20155, Sumatera Utara, Indonesia

<sup>2</sup>Pusat Unggulan Green Chitosan dan Material Maju, Universitas Sumatera Utara, Medan 20155, Sumatera Utara, Indonesia

<sup>3</sup>Department of Physic, Faculty of Mathematics and Natural Sciences, Universitas Sumatera Utara, Medan 20155, Sumatera Utara, Indonesia

<sup>4</sup>School of Materials Engineering, Universiti Malaysia Perlis, Jejawi 02600, Arau, Perlis, Malaysia

**Keywords:** Chitosan-roselle, Thermal Properties, Casting Method, Cure Temperature.

**Abstract:** The chitosan-roselle films were fabricated by casting method. The roselle ratio and cure temperature of films were varied to study the thermal properties of the chitosan-roselle films. Thermal properties of chitosan-roselle films showed higher heat resistance when blend roselle ratio and cure temperature were increased. The temperature at maximum degradation rate of chitosan-roselle films was determined by DTG. The chitosan-roselle films were degrade faster when the roselle ratio increased at ambient temperature. The cure temperature was varied to 50, 60 and 70°C, the most optimum cure temperature was 60°C which showed the lowest weight loss and exhibited the highest heat resistance compared to the other cure temperature. SEM results showed the surface structure of different ratio of chitosan-roselle films which were cure at 50, 60 and 70°C. The surface structure become smoother when the ratio of chitosan-roselle was increased. FTIR result showed that the intensity percentage of functional group exist in pure chitosan films were improved by adding roselle to become chitosan-roselle films. The results showed the most optimum cure temperature was 60°C which showed high intensity percentage compared to the other cure temperature.

## 1 INTRODUCTION

The potential of biopolymers, especially the polymers obtained from renewable resources has long been recognized. In the last decade there has been increasing interest in developing thermoplastic biopolymers, especially those are derived from renewable sources. However, these biopolymers are mostly used in food industry but very less to replace synthetic materials. Packaging based on conventional synthetic materials has brought the threat to ecology. These concerns lead to a need for more effective safety regulations and better system to maintain the quality of the food (Portes, 2009). The biopolymers that are used as coating in food packaging have the advantages to be available from biocompatible, biodegradable and better quality of fresh foods as well as of environmentally friendly packaging. Biomass is a naturally abundant source and has long been recognized as sustainable biopolymers, and in the recent years, growing environmental awareness

has led to studies of biopolymer as alternative packaging films to be used as edible coatings in food packaging (Tharanathan, 2003). This approach will be very interesting from an academic point of view and large-scale usage in the food industry. Biopolymers such as polysaccharides, proteins, lipids and combination of those components are potential to be made as films. Biopolymer films are known as edible films. Edible films have been particularly considered in food preservation because of their capability in improving global food quality (Tharanathan, 2003 and Norashikin, 2010).

Nowadays, the materials most used for packaging are petrochemical based polymers because of their availability in large quantities with low cost and many functional features, such as good tensile strength and tear strength, good barrier properties and heat stability of oxygen. However, these materials are non-biodegradable which lead to very serious ecological and environment pollution problem. As a solution, there is a need to shift to eco-friendly biodegradable materials, especially from renewable agriculture by

products such as chitosan, food processing industry wastes and low- cost natural resources such as starch (Alves, 2006).

In this context, chitin is representing as a second most abundant biopolymer after cellulose (Ou, 2005). Chitosan is a linear amino polysaccharide obtained from the deacetylation of chitin (Portes, 2009) (a process of remove the acetyl function group at chitin), the major structural component of the exoskeleton of invertebrates and the cell walls of some plant like fungi. In addition, in view of the most biopolymers are either biodegradable or compostable, it can also be argued that chitosan could be fit with the 'cradle-to-cradle' concept, which means that on disposal, it could become 'food' for the future generation of materials (Ou, 2005).

Chitosan has biodegradability and biocompatibility properties, and compared with chitin, it shows better solubility in common solvents. This is why chitosan is commonly used in several applications instead of chitin. Chitin and chitosan have applications from cosmetic to pharmaceutical industries and its total annual production estimated at least 1000 tons per year. Due to this variety of applications, there is a necessary to fully understand their molecular nature to increase their uses (Leceta, 2013). Chitosan has been studied as natural antibacterial, bio-based active films and excellent compatibility with other substances by the presence of the high density of amino groups and hydroxyl groups in chitosan polymer structure (Betzabe, 2009 and Ngah, 2011).

Chitosan film can be easily prepared, but it is difficult to handle due to the curving during drying phase, if no assisting means and weight are used to keep it straight (Kammoun, 2013 and Annala, 2007). In general, the properties of chitosan solutions depend on several parameters including ionic strength, concentration, temperature, acid concentration and type of acid. Acetic acid was used in this study since chitosan is soluble in acetic acid (ZhenXing, 2007; Esam, 2010 and Jayakumar, 2007). In this study, roselle was used as admixture to produce chitosan-roselle films. Roselle has unique properties such as ionic liquid forming because it contains of high minerals concentration especially ferrum and minerals enable the blend films are thermally stable. Blends of chitosan and roselle were produced by using acetic acid as a solvent media. Different temperatures which are 50, 60 and 70°C were applied to cure chitosan-roselle films.

Throughout the years, some researches have done some improvement on the performance of biodegradable film in the food packaging area. From

all the points above, an attempt was done to investigate the effect of different chitosan concentration in a composite biodegradable film (Cissé, 2013 and Kumirska, 2010). Chitosan is a linear  $\beta$ -1,4-D-glucosamine is a biocompatible, nontoxic compound mainly obtained by deacetylation of chitin, a natural structural component present for instance in crustaceans. This biopolymer presents interesting properties by excellent film forming capacity and gas and aroma barrier properties at dry conditions, which makes it a suitable material for designing food packaging structure. However, biodegradable films are often have limited temperature resistance (Kammoun, 2013). A simple blend process of the chitosan solution with roselle extract was used to produce the chitosan-roselle which may able to be used to improve the thermal properties of chitosan films.

## 2 MATERIALS AND METHOD

Chitosan powder (medium grade, 99.9% purity) synthesized from crab shell was purchased from Sigma Aldrich Ltd, medium molecular weight). 2% of acetic acid with 99.9% purity (Merck) and methanol (GMBH) were used as solvents in this research. Roselle was extracted by using a mixture of acetic acid, methanol and deionized water with ratio 1:4:5 and it was used as a biomaterial to be blended with chitosan. Chitosan solution gel was prepared by dissolving weighted chitosan powder into 50 ml of acetic acid 2%. The chitosan powder was weighted 1.75 g and pours into 100 ml of acetic acid 2% and then stirred by using a magnetic stirrer with 300 rpm for 12 hours at room temperature to fully dissolve the chitosan powder into the acetic acid. Acetic acid 2% was the most suitable solvent to dissolve chitosan. This is due to chitosan which is soluble in weak acid. Chitosan-roselle solution was prepared by mixing roselle extract with the chitosan solution. First, to prepare roselle extract, the seed of roselle flower was removed to obtain roselle calyces. Then the calyces were washed with tap water to remove unwanted particle and cut into small pieces to be mashed. Then, it was blended into paste follow by extract squeezing into a breaker. A mixture of acetic acid, methanol and deionized water were prepared with ratio 1:4:5. The 50 ml blended roselle juice was added into 50 ml mixture of methanol, acetic acid and deionized water. Then, the mixture was stirred by using a magnetic stirrer with 300 rpm for 30 minutes at room temperature. The well mixed mixture was then filtered by using 125 mm size of filter paper. After the chitosan-roselle solution was prepared, it was poured into a mold

and left it to dry in an oven with different curing temperature which were 50, 60 and 70°C. The film thickness was measured with a 0-25 mm micrometer with an accuracy of  $\pm 0.01$  mm in four random locations for each film. After the solution completely dry into film, several characterizations using Differential Scanning Calorimeter (DSC), Thermogravimetry Analyzer (TGA), Scanning Electron Microscope (SEM) and Fourier Transform Infrared Spectroscopy (FTIR) were performed.

The difference in heat flow of the composite was measured as a function temperature by using Differential Scanning Calorimetry (DSC) which recorded by a NETZSCH DSC 204 F1 (Germany) instrument with standard ASTM D34218 DSC. The onset temperature and degree of crystallinity data was obtained from the DSC thermograms. In this study, DSC was used to determine the possible transition of the chitosan-roselle composite film. The thermogram was run by placing the samples (3-10 mg) in an aluminium pan and a heating scan was conducted from range of 30 to 480°C at a heat rate 10°C/min. Purge gas flow was adjusted to 50 ml/min using nitrogen gas. The mass or changes in mass of the sample as a function of temperature or time both was measured by using Thermogravimetric Analysis (TGA). TGA analysis was conducted according to ASTM D258 standards. The specimens of 10 mg were put in the platinum pan. TGA measures the amount and rate of change in the weight of material as a function of temperature or time in a controlled atmosphere. This technique can characterize materials that exhibit weight loss or gain due to decomposition, oxidation, or dehydration (Dev Raj, 2013). TGA was used to determine the estimated lifetime and weight change in the samples.

Purge gas flow need to be adjusted to 50 ml/min using nitrogen gas. The heating rate was set at 30 to 900°C at 10°C/min. In this study, the surface morphology of chitosan-roselle films were examined by using a Jeol JSM- 6460LA scanning electron microscopy (SEM) at an accelerating voltage of 5 kV. FT-IR spectra measurements were conducted by a Perkin Elmer RX1 FT-IR spectrometer.

### 3 RESULTS AND DISCUSSION

#### 3.1 Making of Charcoal

All films were easily peeled from the film-casting mold. Thin film formation was easy due to the low surface tension on the casting surface. Peeled films were then conditioned at testing temperature to obtain soft, flexible, and easy to handle films. Chitosan-

roselle films were cured at temperature 50, 60 and 70°C.

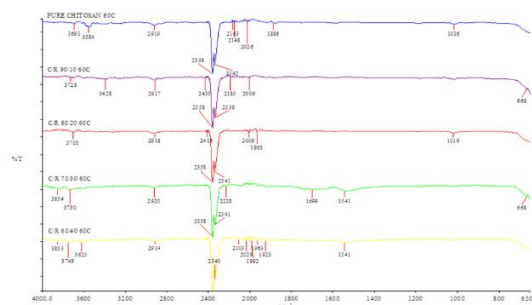


Figure 1: The FTIR spectra of chitosan-roselle films which are cured at 60°C.

FT-IR spectrum was used to identify the chemical structure of chitosan-roselle films by scanning the chitosan-roselle films using FT-IR. The results of FT-IR spectra which were cured at 60°C are reported in Figure 1. The O-H stretching mode of chitosan was observed in the region of 3200–3650  $\text{cm}^{-1}$  where in these spectra pure chitosan falls at 3618  $\text{cm}^{-1}$ . This peak due to overlapping of extension of C-H and O-H in chitosan. The peak at 2395  $\text{cm}^{-1}$  is due to extension of C-H group. The peaks at 2362 and 2339  $\text{cm}^{-1}$  are due to C-N bond. Since the absorption peaks ranges is available until 3650  $\text{cm}^{-1}$ , so the peaks over 3650  $\text{cm}^{-1}$  were assumed as impurities. The peak at 2060 to 1886  $\text{cm}^{-1}$  indicating the existence of Fe-S bond. The presence of the ferredoxin in the structure can improve the thermal properties of the film. The peaks at 1623  $\text{cm}^{-1}$  were the C=O stretching (amide I) and NH bending (amide II). The peak near 1780  $\text{cm}^{-1}$  suggested the presence of a carbonyl group in the chitosan and roselle films. The absorption peaks at 1016 and 1019  $\text{cm}^{-1}$  were probably due to the C-O-H bending mode. Clear differences can be detected in the infrared spectra of chitosan and roselle, both in the different absorbance values and shapes of the bands and in their location. A decrease in the intensity of the O-H absorption band at 3323  $\text{cm}^{-1}$  was observed, indicating that the hydroxyl group contents in roselle. The lower xylan content in roselle was proved by a weak carbonyl band at 1699  $\text{cm}^{-1}$ . The enhanced carbonyl absorption peak at 1779  $\text{cm}^{-1}$  (C=O ester), C-H absorption at 1381  $\text{cm}^{-1}$  (C-CH<sub>3</sub>), and C-O stretching band at 1242  $\text{cm}^{-1}$  confirmed the formation of ester bonds. Also, it was proved by an increase in the intensity of OH in plane bending vibration at 1366  $\text{cm}^{-1}$  band specific to the component cellulose and hemicelluloses. A small band at 16243  $\text{cm}^{-1}$  were assigned to the absorbed water and  $\beta$ -glucosidic linkages between the sugar units,

respectively. Weak absorptions between 1500 and 1400  $\text{cm}^{-1}$  arose from the aromatic ring vibrations and ring breathing with C–O stretching in lignin.

Figure 2 shows curve of weight loss (%) as a function of temperature for chitosan-roselle films which are cured at 50 °C with heating rate of 10 °C/min in the temperature range from room temperature to 980 °C. All ratio of chitosan-roselle films almost have similarity in the shape of the curves, but magnitudes of weight loss is varied. The initial weight loss for all the samples starts near 100 °C, the loss of weight is about 10%, as a result of removing the adsorbed water on the composite and loss of bound water and acetic acid from the composites. The weight increase in the range of 33 to 70 °C is because of the reaction between chitosan and roselle at ratio 60:40. It was, however, much smaller than the weight loss in the range of 70 to 120 °C and then the weight increases almost disappeared. The weight loss in the second starts in range 82.13–86.05 °C and continues up to 280 °C of melting temperature,  $T_m$ . There was about 40% weight loss was due to the decomposition of blend. The third weight loss was observed in the range 66.35–67.69 °C which probably due to the structural decomposition of the blend caused by the loss of water. There was about 70% weight loss and it may be referred to a complex process including the dehydration of the saccharide rings and depolymerization. As would be expected, the higher the gas temperature, the faster the heating rate and the more rapid and weight loss is increase. The TGA curves for the chitosan-roselle films with ratio 90:10 and 60:40 illustrated similar patterns of weight loss, however, chitosan-roselle films with ratio 50:50 exhibited a greater weight loss than the other samples at temperature around 290 °C. It was observed that the weight loss of chitosan-roselle films with ratio 60:40 was the highest at first until  $T_m$ . It is probably due to the easy of chitosan-roselle to react with each other. After passed the  $T_m$ , the weight loss of other ratio was higher than it. The chitosan-roselle films of ratio 90:10 and 50:50 were more resistance to heat before reach  $T_m$  and rapidly degrade after reach  $T_m$ . At this cure temperature, chitosan-roselle film with ratio 90:10 showed great thermal resistance properties than other ratios. The peaks of chitosan-roselle blend films were very weak around temperature 600 °C may be due to the desorption of the adsorbed water on the sample when it was kept overnight. It can be seen that the DTGA curves and the maximum peaks temperature shifted as the heating rate increases. An increase of the heating rate tended to delay thermal decomposition process towards higher temperatures, most probably due to heating rate implies that the

material reaches that temperature in a shorter time. According to the results, the yield of chitosan-roselle films at about 20% and the behavior of TGA curves were almost similar in the composites films (Figure 2-Figure 7).

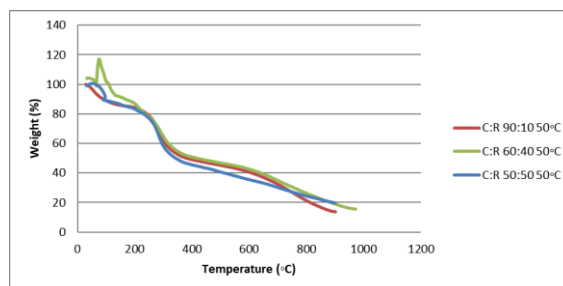


Figure 2: TGA curves for thermal decomposition of chitosan-roselle films at 50 °C.

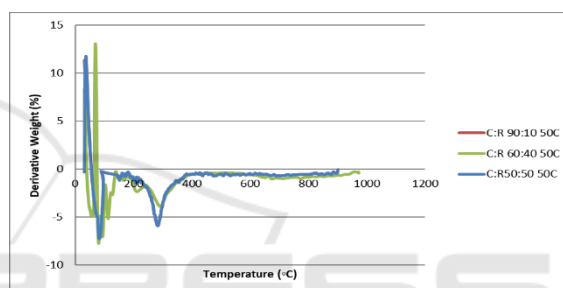


Figure 3: DTGA curves for thermal decomposition of chitosan-roselle films at 50 °C.

Figure 3 shows curve of weight loss (%) as a function of temperature for chitosan-roselle films which cured at 60 °C with heating rate of 10 °C/min in the temperature range from room temperature to 980 °C. From the Figure 2-7, all ratio of chitosan-roselle films almost have similarity in the shape of the curves, but magnitudes of weight loss were varied. The initial weight loss for all samples at approximately 100 °C is around 10%. This may due to the evaporation of water and due to the loss of water content and acetic acid from the composite. The weight loss in the second range started around 180 °C and continued up to 253 °C melting temperature,  $T_m$ . The weight loss third stage observed in the range 255 °C corresponds to structural decomposition of the blend which there was about 66% weight loss of the original sample. It was observed that the weight loss of chitosan-roselle films with ratio 60:40 was highest than others ratio. Combination of chitosan-roselle improved the thermal properties of chitosan film at cure temperature 60 °C. This ratio was more resistance to heat before reach  $T_m$  and rapidly degraded after reach  $T_m$ . At this cure temperature, chitosan-roselle



with ratio 60:40 showed great thermal resistance properties than other ratios. According to the results, the char yield of chitosan-roselle films at about 14% and the behavior of TGA curves were almost similar in the composites films (Figure 2-Figure 7). The results showed that, the char yield of chitosan:roselle at all ratio were less which were between 15% and 17% respectively. Therefore, the addition of roselle can improve the thermal stability of chitosan-roselle films. It was found that the char yield of chitosan-roselle film was enhanced as addition of roselle in chitosan-roselle composite. These results means high thermal stability of chitosan-roselle films.

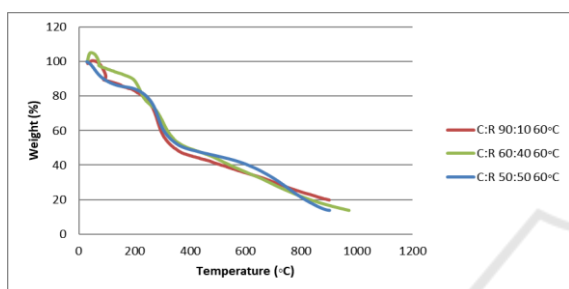


Figure 4: TGA curves for thermal decomposition of chitosan-roselle films at 60°C.

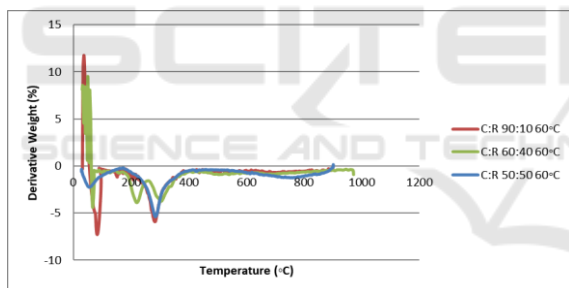


Figure 5: DTGA curves for thermal decomposition of chitosan-roselle films at 60°C.

Figure 6 shows curve of weight loss (%) as a function of temperature for chitosan-roselle films which cured at 70°C with heating rate of 10°C/min in the temperature range room temperature to 980°C. From the Figure 7, the initial weight loss for all samples at approximately 100°C was around 10%. This may due to the evaporation of water and due to the loss of water content and acetic acid from the composite. The weight loss in the second range started around 202.5°C which was referred to combustion of cellulose from roselle. The weight loss third stage found in range 255-463.1°C corresponds to a complex process including the dehydration of the saccharide rings and depolymerization. The TGA curves showed that chitosan-roselle composite films

slowly decline above 350°C with a maximum rate of decomposition occurring at about 300-340°C.

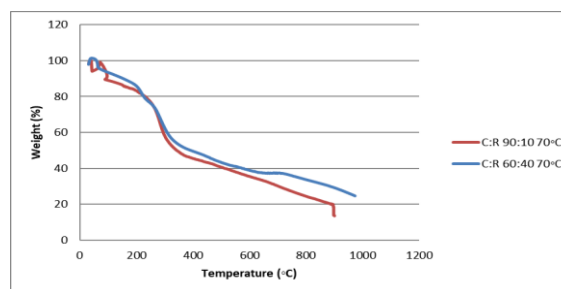


Figure 6: TGA curves for thermal decomposition of chitosan-roselle films at 70°C.

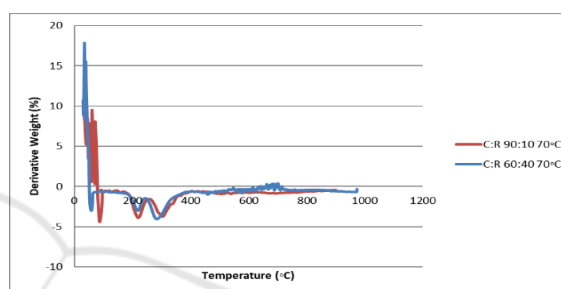


Figure 7: DTGA curves for thermal decomposition of chitosan-roselle films at 70°C.

Table 1: The thermal decomposition of chitosan-roselle films.

Sample	Temperature Decomposition (°C)		Weight loss (%)	
	2 <sup>nd</sup> stage at	3 <sup>rd</sup> stage	2 <sup>nd</sup> stage at	3 <sup>rd</sup> stage
	C:R 90:10 50°C	132.4	193.8	17.87
C:R 60:40 50°C	203	259	16.85	35.97
C:R 90:10 60°C	180	233.1	32.55	34.55
C:R 60:40 60°C	197	274	17.63	32.96
C:R 90:10 70°C	202.5	-	27.06	-
C:R 60:40 70°C	191	255	15.62	33.27

Differential scanning calorimeter (DSC) measurements were performed to estimate the thermal transition of chitosan-roselle films by ratio 90:10 and 60:40 of chitosan-roselle at different testing temperature. All the samples were heated from room temperature to 480°C and rate of 10° C/min. The DSC glass transitions are shown in Figure 8-10. Figure 8 shows thermal transition of the chitosan-

roselle films in cure temperature 50°C. Figure 8 does not show any peak for glass transition temperature. It shows crystallization and melting point chitosan-roselle films as stated in the Table 1. Chitosan-roselle films showed an endothermic peak at around 94.48 to 98.33°C associated with the dehydration (loss of water associated with the hydrophilic groups of the polymer) in film matrix. The exothermic peak which appears in the temperature ranges about 279.45 and 281.89°C corresponds to the decomposition of the polymer. Based on the previous research, the thermal degradation of chitosan begins at about 250°C. The exothermic can be explained through the crystallization of chitosan. The melting point of chitosan-roselle films were 212.85 and 209.96 °C respectively following the ratio. These peak temperatures tend to shift to lower temperatures with increased roselle concentration. In crystalline molecules of original chitosan was packed in a way that their interactions are strongest. When the chitosan was blended, it stretches the crystal lattice, molecules are not in the optimal positions and their interactions are weaker, thus less energy is required to break them. At cure temperature 50°C, chitosan-roselle films with ratio 60:40 showed the highest melting temperature while 90:10 showed the lowest melting temperature.

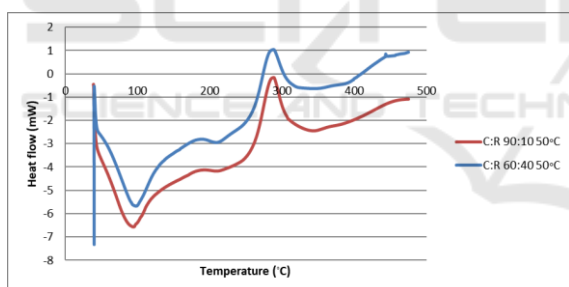


Figure 8: The DSC glass transitions of chitosan-roselle films at 50°C.

Thermal transition of the chitosan: roselle films were affected by different ratio of chitosan and roselle in cure temperatures 60°C as shown in Figure 9. The sample were heated from room temperature to 480°C at a rate of 10°C/min. Chitosan-roselle films exhibited a broad endothermic peak at 91.59°C and 85.82°C respectively following the ratio because of the dehydration (loss of water associated with the hydrophilic groups of the polymer) in the films. The exothermic peak which appeared in the temperature ranges at 287.91 and 302.34°C corresponds to the decomposition of the polymer. Based on the previous research, the thermal degradation of chitosan begins at about 250°C. The exothermic can be explained

through the crystallization of chitosan. The melting point of chitosan-roselle films were 214.77 and 216.69°C respectively following the ratio. In crystalline molecules of original chitosan was packed in a way that their interactions are strongest. When the chitosan is blended, it stretches the crystal lattice, molecules are not in the optimal positions and their interactions are weaker, thus less energy is required to break them. At cure temperature 60°C, chitosan-roselle films with ratio 60:40 showed the highest melting temperature while 90:10 showed the lowest melting temperature. When compare the result of cure temperature of 60°C with other two cure temperature, it showed the highest melting temperature. In other meaning, 60°C is the most optimum temperature to produce high melting temperature (heat resistance films).

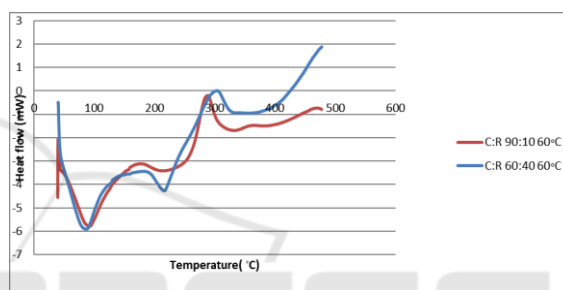


Figure 9: The DSC glass transitions of chitosan-roselle films at 60°C.

Thermal transition of the chitosan-roselle films were affected by different ratio of chitosan and roselle in cure temperatures 70°C as shown in Figure 10. The sample were heated from room temperature to 480°C at a rate of 10°C/min. Chitosan-roselle films exhibited a broad endothermic peak at 84.85 and 88.7°C respectively following the ratio because of the dehydration (loss of water associated with the hydrophilic groups of the polymer) in the films. The exothermic peak which appeared in the temperature ranges at 303.31 and 307.99°C corresponded to the decomposition of the polymer. Based on the previous research, the thermal degradation of chitosan begins at about 250°C. The exothermic can be explained through the crystallization of chitosan. The melting point of chitosan-roselle films were 215.73 and 208.03°C respectively following the ratio. In crystalline molecules of original chitosan was packed in a way that their interactions are strongest. When the chitosan was blended, it was stretched the crystal lattice, molecules are not in the optimal positions and their interactions are weaker, thus less energy is required to break them. At cure temperature 70°C, chitosan-roselle films with ratio 60:40 showed the

highest melting temperature while 90:10 showed the lowest melting temperature. When compare the result of cure temperature of 70°C with other two cure temperature, it showed the lowest melting temperature.

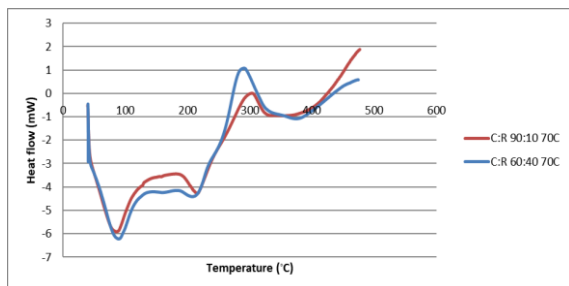


Figure 10: The DSC glass transitions of chitosan-roselle films at 70°C.

Table 2: The melting temperature of chitosan-roselle films.

Sample name	Crystallization temperature (°C)	Melting temperature (°C)
C:R 90:10 50°C	94.48	212.85
C:R 60:40 50°C	98.33	209.96
C:R 90:10 60°C	91.59	216.77
C:R 60:40 60°C	85.82	214.69
C:R 90:10 70°C	84.85	215.73
C:R 60:40 70°C	88.70	208.03

Scanning Electron Microscopy (SEM) was used to study the surface morphology of the chitosan-roselle films. There are 4 magnification used which are x100, x250, x500 and x2000. The morphology of chitosan-roselle films which cured at 60°C are reported in Figure 11. SEM images for chitosan-roselle films with ratio 100:0 and 90:10 showed the largest rough surface. The surface of chitosan films was smooth and not homogenous due to the present of phase separation. Roselle did not disperse well within the chitosan matrix in the blend films. Chitosan-roselle films with the ratio of 80:20, 70:30 and 60:40 had smoother surface than chitosan-roselle films with ratio 100:0 and 90:10. From the micrograph under magnification, the surface of chitosan-roselle films became smoother as the ratio of chitosan-roselle films decreased. This may be due to chitosan-roselle films particles have failed to crystallize.

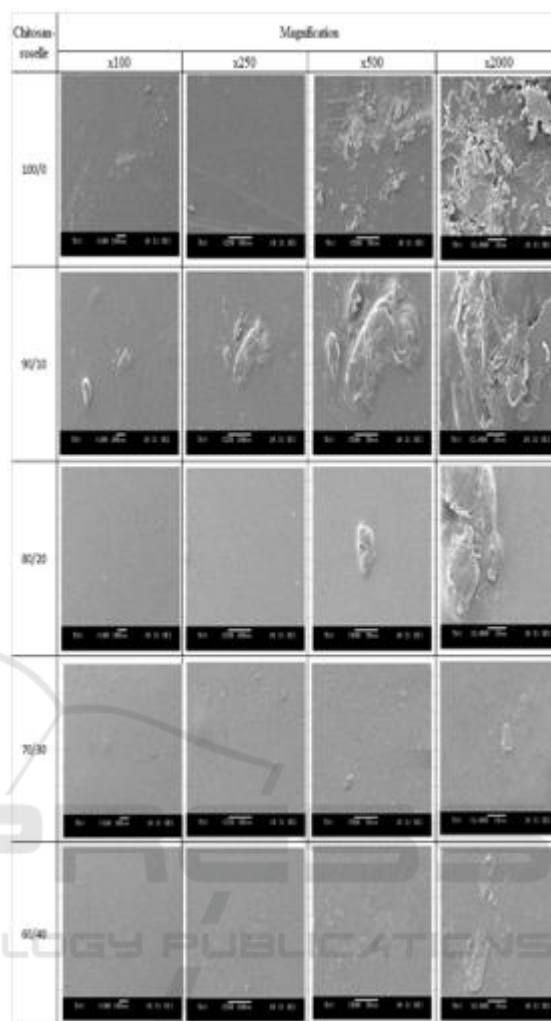


Figure 11: SEM images of chitosan-roselle films which cured at 60°C.

## 4 CONCLUSIONS

FTIR result showed that the intensity percentage of functional group exist in pure chitosan films were improved by adding roselle to become chitosan-roselle films. Besides, it showed the most optimum cure temperature was 60°C which showed high intensity percentage compared to other cure temperature (50 and 70°C). From the thermal testing (TGA, DTG, and DSC), the melting temperature of chitosan-roselle films showed higher melting temperature when increase the roselle ratio in the blend films at cure temperature 50, 60 and 70°C. This means that chitosan-roselle films showed higher heat resistance when ratio of roselle increased. The temperature at maximum

degradation rate of chitosan-roselle films determined by DTG were lower when increased the roselle ratio in the blend films at cure temperature of 50, 60 and 70°C. Thus, the chitosan-roselle films were degrade faster when increased the roselle ratio in blend film at ambient temperature. From the cure temperature 50, 60 and 70°C, the most optimum cure temperature was 60°C which showed the lowest weight loss and exhibited the highest heat resistance compared to other cure temperature. SEM results showed the surface structure of different ratio of chitosan-roselle films which were cure at 60°C. The higher ratio of chitosan-roselle, the surface structure become smoother. As conclusion, chitosan-roselle films have higher heat resistance, degraded faster and have smoother surface at most optimum cure temperature (60°C). The smoother surface of chitosan-roselle films made the higher thermal resistance of these blend films.

## ACKNOWLEDGEMENTS

This work was supported by Faculty of Mathematic and Natural Sciences, Universitas Sumatera Utara and School of Materials Engineering, Universiti Malaysia Perlis.

## REFERENCES

- Alves, V., Costa, N., Hilliou, L., Larotonda, F., Gonçalves, M., Sereno, A., & Coelho, I., 2006. Design of biodegradable composite films for food packaging. *Desalination*, 199(1-3), 331-333.
- Betzabe Gonza Lez-Campos, Evgen Prokhorov, Gabriel Luna-Bárcenas, Abril Fonseca-García, & Isaac C.Sanchez., 2009. Dielectric relaxations of chitosan: The effect of water on the  $\alpha$ -relaxation and the glass transition temperature. *Journal of Polymer Science Part B Polymer Physic*, 47(22), 2259-2271.
- Cissé M., Kouakou A.C., Montet D., Loiseau G., Ducamp-Collin M.N., 2013. *Food Hydrocolloids*, 30 (2), 576-580.
- Dev Raj. and J. Yamini, 2013. Preparation and Characterization of Pharmaceutical Grade Chitosan and Hydrated Chitosan Gums for Topical Preparations. *Chem. Phys Journal*. 1(9), 858-860.
- Esam A. El-hefian and Abdul H. Yahaya., 2010. Rheological study of chitosan and its blends: An overview of chitosan, *International Journal of Carbohydrate Chemistry* 4(02), 210-220
- Portes, E., Gardrat, C., Alain, C., & Véronique, C., 2009. Environmentally friendly films based on chitosan and tetrahydrocurcuminoid derivatives exhibiting antibacterial and antioxidative properties. *Carbohydrate polymers*. 76(4), 578-584.
- Jayakumar, N. Nwe, S. Tokura, H. Tamura, 2007. Sulfated chitin and chitosan as novel biomaterials. *International Journal of Biological Macromolecules*, 40(3), 175-181
- Kammoun, M., Haddar, M., Kallel, T. K., Dammak, M., & Sayari, A., 2013. Biological properties and biodegradation studies of chitosan biofilms plasticized with PEG and glycerol. *International Journal of Biological Macromolecules*.
- Kumirska, Jolanta., Czerwicka, M., Kaczyński, Z., Bychowska, A., Brzozowski, K., Thoming, J., & Stepnowski, P., 2010. Application of Spectroscopic Methods for Structural Analysis of Chitin and Chitosan. *Marine Drugs*. 8(5), 1567-636.
- Leceta, I., Guerrero, P., Ibarburu, I., Dueñas, M.T., de la Caba, K., 2013. Characterization and antimicrobial analysis of chitosan-based films. *Journal of Food Engineering*, 116,(2013), 889-899.
- Ngah, W.S.W., Fatinathan, S. and Yosop, N.A., 2011. Isotherm and kinetic studies on the adsorption of humic acid onto chitosan-H<sub>2</sub>SO<sub>4</sub> beads. *Desalination*. 272, 293-300.
- Norashikin, M. I., 2010. Fabrication and Characterization of Sawdust. *World Academy of Science, Engineering and Technology*, 716-719.
- Ou, Y. Wang, S. Tang, C. Huang, and M. G. Jackson, 2005. "Role of ferulic acid in preparing edible films from soy protein isolate," *Journal Food Eng*, vol. 70, pp. 205-210.
- Tharanathan, R. N., 2003. Biodegradable films and composite coatings: past, present and future. *Trends in Food Science and Technology*, 14, 71-78.
- Tuija Annala, 2007. Chitosan Film Preparation, Instruction for laboratory experiments, Rev 0.
- ZhenXing Tang, and JunQinQin, 2007. Use of chitosan gel for the purification of protein, *Engineering AND Technology*, College of Chemical Engineering and Materials Science, Zhejiang University of Technology, Hangzhou, Zhejiang, China.